Available at www.sciencedirect.com

ScienceDirect

journal homepage: www.elsevier.com/locate/he

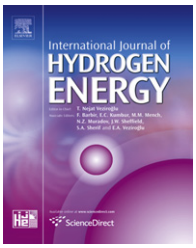

Hydrogen production with nickel powder cathode catalysts in microbial electrolysis cells

Priscilla A. Selembo [a,1], *Matthew D. Merrill* [b,1], *Bruce E. Logan* [b,*]

[a] *Department of Chemical Engineering, Pennsylvania State University, University Park, PA 16802, USA*
[b] *Department of Civil and Environmental Engineering, Pennsylvania State University, University Park, PA 16802, USA*

ARTICLE INFO

Article history:
Received 2 October 2009
Received in revised form
28 October 2009
Accepted 3 November 2009
Available online 24 November 2009

Keywords:
MEC
Electrohydrogenesis
Hydrogen production
Cathode
Metal
Nickel

ABSTRACT

Although platinum is commonly used as catalyst on the cathode in microbial electrolysis cells (MEC), non-precious metal alternatives are needed to reduce costs. Cathodes were constructed using a nickel powder (0.5–1 μm) and their performance was compared to conventional electrodes containing Pt (0.002 μm) in MECs and electrochemical tests. The MEC performance in terms of coulombic efficiency, cathodic, hydrogen and energy recoveries were similar using Ni or Pt cathodes, although the maximum hydrogen production rate (Q) was slightly lower for Ni (Q = 1.2–1.3 m^3 $H_2/m^3/d$; 0.6 V applied) than Pt (1.6 m^3 $H_2/m^3/d$). Nickel dissolution was minimized by replacing medium in the reactor under anoxic conditions. The stability of the Ni particles was confirmed by examining the cathodes after 12 MEC cycles using scanning electron microscopy and linear sweep voltammetry. Analysis of the anodic communities in these reactors revealed dominant populations of *Geobacter sulfurreduces* and *Pelobacter propionicus*. These results demonstrate that nickel powder can be used as a viable alternative to Pt in MECs, allowing large scale production of cathodes with similar performance to systems that use precious metal catalysts.

1. Introduction

Most current hydrogen production methods use processes such as steam reforming and coal gasification that rely on non-renewable energy sources [1]. Electrohydrogenesis using microbial electrolysis cells (MEC) is a promising approach for hydrogen production from organic matter, including wastewater and other renewable resources [2,3]. In an MEC, exoelectrogenic bacteria oxidize organic matter into CO_2, electrons, and protons. The bacteria transfer electrons from the oxidation reaction to the anode and release protons to the solution. Hydrogen gas is formed by the reaction between electrons and protons at the cathode, achieved by adding a supplemental voltage (0.114 V in theory for acetate as the substrate) to that produced by the bacteria (≥0.2 V) to overcome the endothermic barrier of hydrogen formation (0.414 V).

Most MEC research has been done using cathodes containing a Pt catalyst, with the Pt accounting for the greatest percentage of the cost of the MEC electrodes [2,4,5]. The high cost of Pt and its susceptibility to poisoning has led researchers to examine non-precious metals and alternatives. MECs with stainless steel (SS) brush cathodes (type 304) produced hydrogen (Q = 1.7 $m^3/m^3/d$), applied voltage of

* *Corresponding author*. Tel.: +814 863 7908; fax: +814 863 7304.
E-mail addresses: pag8@psu.edu (P.A. Selembo), merrill@engr.psu.edu (M.D. Merrill), blogan@psu.edu (B.E. Logan).
[1] Tel.: +814 865 9387; fax: 814 863 7304.

0360-3199/$ – see front matter © 2009 Professor T. Nejat Veziroglu. Published by Elsevier Ltd. All rights reserved.
doi:10.1016/j.ijhydene.2009.11.014

$E_{ap} = 0.6$ V at rates similar to those containing platinum ($Q = 0.5$–2.0 $m^3/m^3/d$) due to the catalytic activity of the SS and the increased surface area of the brush [6]. Electrodeposited nickel alloys (NiMo and NiW) were used in MEC cathodes that produced hydrogen at a rate of $Q = 2.0$ $m^3/m^3/d$ ($E_{ap} = 0.6$ V) [7]. An MEC with a cathode lacking a metal catalyst produced hydrogen at a lower rate of $Q = 0.57$ $m^3/m^3/d$ and higher applied voltage of $E_{ap} = 1$ V [8]. MECs with biocathodes have also shown promise, achieving $Q = 0.63$ $m^3/m^3/d$ at $E_{ap} = 0.7$ V [9]. Tungsten carbide was recently examined as a catalyst for hydrogen production under neutral pH conditions [10], but it was not evaluated in an MEC.

Nickel, nickel alloys, and SS are widely used as cathodes for alkaline water electrolysis due to their relatively good catalytic activity, high corrosion stability, and low cost [11]. Their performance has been well studied using various electrochemical techniques, such as cyclic voltammetry and linear sweep voltammetry (LSV), but only under alkaline conditions [12–18] or at high temperatures. High temperatures (450–700 °C) are used for hydrogen production by the water-gas shift reaction from carbon monoxide [19] or steam reforming [20]. MECs typically operate at neutral pHs and at temperatures (20–30 °C) suitable for microbial growth. Thus, the hydrogen evolution activity of metal catalysts needs to be better understood under these less optimum conditions.

Flat sheet metal cathodes made from stainless steel and Ni have been shown to perform similar to, or better than, Pt sheet cathodes based on LSV scans and MEC tests under neutral pH conditions and ambient temperatures [21]. Electrodeposition of nickel oxide onto the stainless steel and nickel alloy surfaces improved performance to $Q = 0.76$ $m^3/m^3/d$ from $Q = 0.01$–0.1 $m^3/m^3/d$ (no Ni oxide) at $E_{ap} = 0.6$ V. While these studies are useful for understanding the performance of materials under well defined conditions, it is not necessary to construct the electrode from one solid piece of material. For example, the Pt used in MEC cathodes consists of nano-sized particles in order to minimize total mass of the material, and thus material costs.

In this study, we constructed cathodes made with commercially-available nickel and SS powders with different sizes at different metal loadings, and compared their performance to platinum powder cathodes. The various cathodes were screened for their performance in neutral pH solutions and at 30 °C using LSV. The most promising cathodes, based on the lowest overpotentials in LSV scans, were then tested in single-chamber MECs for hydrogen gas production.

2. Materials and methods

2.1. Cathodes

Commercially-available metal powders of nickel (2–10 μm), nickel oxide NiO_x 87302 (≤74 μm), and stainless steel catalysts (≤140 μm) were obtained from Alfa-Aesar, MA. Filamentous nickel powders with smaller particle sizes were obtained from INCO specialty products, NJ (Ni 210: 0.5–1 μm, Ni 110: 1–2 μm and Ni 255: 2.2–2.8 μm; all >99% pure). Cathodes were made by mixing the metal powder with Nafion™ binder (Sigma-Aldrich, MO), and applying the mixture using a brush onto carbon cloth (surface area 7 cm^2, 30% wet proof, BASF Fuel Cell, NJ). Platinum catalyst was used as a control (0.002 μm) (10 wt% on Vulcan XC-72; BASF Fuel Cell, NJ).

Nickel oxide was electrodeposited ($eNiO_x$) on carbon cloth by applying 20 V at ~1.5 A for 40 s (1696 power source, B&K Precision, USA) with an anode stainless steel brush (SS type Cronifer 1925 HMo, made in house) in a solution containing 18 mM $NiSO_4$ and 35 mM $(NH_4)_2SO_4$ at a pH = 2.0 (adjusted by adding H_2SO_4) [21,22]. Carbon cloth cathodes were prepared before electrodeposition by applying a base coat of carbon black (CB, 5 mg/cm^2) and Nafion ™ (33 μL/cm^2).

2.2. Electrochemical evaluation of catalysts

Performance of the cathodes was evaluated by LSV using a potentiostat (PC4/750TM, Echem Analyst, v. 5.5, Gamry Instruments, PA). The cathodes were placed in electrochemical cells (4 cm long by 3 cm diameter) with an Ag/AgCl reference electrode and platinum wire counter electrode in 2 mM phosphate buffer solution (pH 7.0). LSV scans from −0.4 to −1.4 V with IR compensation (to compensate for the ohmic drop between the working and reference electrode) were repeated three times, at a scan rate of 2 mV/s.

2.3. MEC reactor construction

Single-chamber MECs made of Lexan were 4 cm long containing 3 cm diameter cylindrical-shaped chambers [23]. Anodes were ammonia-treated graphite fiber brushes (25 mm diameter × 25 mm length, 0.22 m^2 surface area) made with a titanium wire twisted core [24,25]. The anodes were first enriched with bacteria in microbial fuel cells (MFCs) containing conventional Pt catalyst air cathodes [26] that were inoculated using a solution from an acetate-fed MFC reactor that had been running for over two years [27]. Duplicate reactors were operated in fed-batch mode using acetate (1 g/L) and a 50 mM phosphate buffer nutrient medium (pH 7) [28] in a 30 °C temperature room. After at least three repeatable cycles, the MFCs were modified to function as MECs by replacing the cathodes and sealing the end of the reactors from air, providing an oxygen-free environment. The voltage needed for MECs was supplied via an external power source (3645A; Circuit Specialists, Inc, Arizona). After each fed-batch cycle (when gas production stopped), the reactors were drained, exposed to air for 15 min to minimize growth of methanogens [23] (except as noted), refilled with substrate solution, and sparged with ultra high purity nitrogen gas for 5 min. For tests done under complete anaerobic conditions, the reactors were drained and refilled inside an anaerobic glove box (N_2/H_2 volume ratio of 95/5). In this case, it was not necessary to sparge the reactors with nitrogen.

2.4. Analysis after MEC cycles

Continuous gas production was measured using a respirometer (AER-200, Challenge Technology, AZ), with the gas collected in gas bags (100 ml capacity, Cali-5 bond, Calibrated Instruments Inc., NY). The composition of the gas in the MEC headspace and gas bags was analyzed using two gas chromatographs (models 8610B and 310, SRI Instruments, CA) with

molesieve columns (5A 80/100, Alltech, IL) and thermal conductivity detectors. Argon was used as the carrier gas for H_2, O_2, N_2 and CH_4 analysis, and helium was used as the carrier gas for CO_2 analysis.

Cathodes were examined using scanning electron microscopy/energy dispersive X-ray spectroscopy (SEM-EDS) at 20 kV (Quanta 200, FEI, OR). Soluble nickel was analyzed via inductively coupled plasma atomic emission spectroscopy (ICP-AES; Optima 5300DV, Perkin-Elmer, MA) at a detection limit of 0.01 ppm. Surface area was obtained by multipoint BET (Brunauer, Emmett, and Teller) based on nitrogen adsorption (ASAP 2020, Micromeritics, GA).

2.5. Calculations

The calculated total geometric surface area of the catalyst particles in the cathodes, $A_{b,p}$ (m^2), is:

$$A_{b,p} = \frac{A_p m}{V_p \rho_{b,p}} = \frac{4\pi r^2 m}{4/3\pi r^3 \rho_{b,p}} = \frac{3m}{\rho_{b,p} r} \quad (1)$$

where A_p is the surface area of a single particle; V_p the volume of particles calculated using the average particle radius, r; $\rho_{b,p}$ the bulk density of the particle (provided by the manufacturer); and m the mass of catalyst added to the cathode.

The performance of the MEC reactors was evaluated as previously described [2,21] in terms of: coulombic efficiency (CE) (%) based on total coulombs recovered compared to the initial mass of substrate; cathodic hydrogen recovery ($r_{H_2,cat}$) (%) or the recovered electrons as hydrogen compared to the current transferred; overall hydrogen recovery ($r_{H_2,COD}$) (%), defined as the percentage of hydrogen recovered compared to the theoretical maximum based on added substrate; volumetric current density (I_V) (A/m^3), calculated from the maximum current production over a 4-h period normalized to the volume of solution; volumetric hydrogen production rate (Q) ($m^3\,H_2/m^3/d$) based on hydrogen gas produced normalized to the reactor volume; energy recovery relative to electrical input (η_E) (%); and overall energy recovery (η_{E+S}) (%) based on both electrical input and heat of combustion of the substrate ($\Delta H_{facetate} = 870.28$ kJ/mol).

2.6. Community analysis

Community analysis of the anode biofilm was performed at the end of 12 cycles for an MEC containing either a Ni or Pt catalyst cathode. Community analysis was not performed on the cathode community as there was no visible biofilm on the electrode surface. Bacteria were extracted from the anode by cutting fibers from the brush using sterile scissors, and vortexing them in sterile buffer with glass beads. The DNA was extracted using Power Soil DNA isolation kit (MoBio laboratories, CA). The 16S rRNA gene fragment of the extracted DNA was amplified by PCR using 27F (5′-AGAGTTTGATCCTGGCTCAG-3′) and 1541R (5′-AAGGAGGTGATCCAGCC-3′) universal primers. Amplified fragments were purified with a QIAquick PCR purification kit (Qiagen, JAPAN), and cloned into *Escherichia coli* competent cells (TOPO TA cloning kit, Invitrogen, MD). Plasmids were extracted using the spin protocol of the EZ96 Fastfilter kit (Omega Bio-tek, GA). Forty-six plasmids from each sampled reactor were sequenced with the T7 primer on the TOPO plasmid (ABI 3730XL DNA Analyzer, Applied Biosystems, CA). Database searches for related gene sequences were conducted through the GenBank nucleotide sequence database using the BLAST algorithm (http://www.ncbi.nlm.nih.gov/BLAST/). The sequences of 16S rRNA genes were aligned and used to generate a phylogenetic tree using the MEGA 4.0.2 program, neighbor-joining method with bootstrap test (500 replicates). Only closest matches (≥90% similarity) were included.

3. Results

3.1. Cathode selection by LSV

An MEC with a Pt catalyst typically produces 4–6 mA, or 0.6–0.9 mA/cm^2 (7 cm^2 cathode projected surface area). Overpotentials for metal catalysts of different sizes and loadings, and with different amounts of binder, were compared at a current density in this range (−0.63 $mA/cm^2 = -3.2$ log A/cm^2) to better predict their performance relative to MEC conditions (Table 1). Both Ni 210 on carbon cloth (60 mg Ni, 267 μL Nafion) and the standard Pt cathode (10 mg Pt, 400 μL Nafion) had the same low overpotential of −0.500 V at this current density (Table 1). Current densities produced with these two materials were also very similar over the complete range of applied voltages (Fig. 1).

Table 1 – Overpotentials vs SHE at current density of −3.2 log A/cm^2 for cathodes during third LSV scan at 2 mV/s. Surface area calculated using Eq. (1), NA – not applicable, ND- not determined.

Catalyst	Particle size (μm)	Surface Area (m^2)	Qty (mg)	CB (mg)	Nafion (μL)	Potential (V)
None (CB)	NA	0.00	0	60	400	−0.970
Platinum	0.002	1.45	10	50	400	−0.500
Ni 210	0.5–1	0.60	60	0	267	−0.500
Ni 210	0.5–1	0.60	60	0	300	−0.583
Ni 210	0.5–1	0.60	60	0	325	−0.713
Ni 210	0.5–1	0.60	60	0	375	−0.713
Ni 210	0.5–1	0.60	60	0	400	−0.720
Ni 210	0.5–1	0.60	60	30	400	−0.668
Ni 110	1–2	0.17	60	30	400	−0.720
Ni 255	2.2–2.8	0.23	60	30	400	−0.721
Ni 10255	2.2–3	0.24	60	30	400	−0.760
Ni 10256	3–7	0.03	60	30	400	−0.739
Ni 210	0.5–1	0.45	30	0	400	−0.747
Ni 210	0.5–1	1.35	90	0	400	−0.727
Ni 210	0.5–1	0.45	30	30	400	−0.683
Ni 10255	2.2–3	0.23	60	0	400	−0.760
Ni 10256	3–7	0.03	60	0	400	−0.740
NiO_x 87302	74	0.001	60	0	400	−1.110
$eNiO_x$	0.001	ND	ND	60	400	−0.800
SS 316	16	0.01	60	0	400	−1.140
SS 316	150	0.002	120	0	400	−0.863
SS 410	150	0.002	120	0	400	−0.913
SS 304	150	0.002	120	0	400	−0.813
SS 303	150	0.002	120	0	400	−0.953

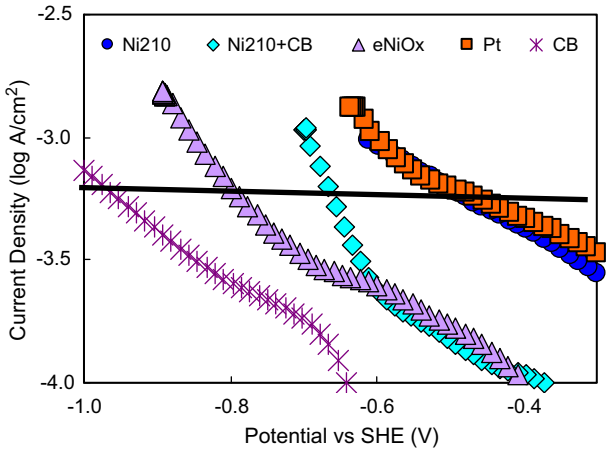

Fig. 1 – Tafel plots for select experimental cathodes in 2 mM phosphate buffer, scan rate 2 mV/s, third scan.

Increasing the amount of binder added to the cathode from 267 μL to 400 μL reduced performance, while changing the mass of Ni added to the cathode (60–90 mg, with 400 μL of binder) did not improve performance of Ni 210. Increasing the surface area was expected to improve current density [29]. This suggests that the effective Ni surface area was not increased when more Ni was added for tests with the higher volume of binder (400 μL). This also may explain why increasing the volume of Nafion binder increased overpotentials, as this likely resulted in less available surface area of the Ni due to increased coverage of the Ni by the binder.

The addition of 30 mg of CB lowered the overpotential of Ni 210 to −0.668 V from −0.720 V at the same Ni (60 mg) and Nafion loading (400 μL). LSV scans when CB was added to Ni with other particle sizes (Ni 10255 and 10256), however, did not show any changes in the current densities across the range of potentials examined. CB may have affected the catalytic activity of the Ni 210 cathode by increasing surface area, improving the application of the metal/binder layer due to the carbon's increased porosity, and increasing chemical stability. Addition of carbon did not change the conductivity of the prepared cathodes (Pt: 1.2 Ω, Ni: 1.1 Ω, Ni + CB: 1.1 Ω), based on measurements with a handheld multimeter (Fluke 87 V True RMS Multimeter, Everett, WA) of the dry electrode before it was placed in the MEC.

In general, a decrease of particle size lowered the cathode overpotential for the smaller particle sizes (0.5–3 μm) but not for the larger particles (3–7 μm). This lack of direct relationship between particle size and current densities was also observed by others using cyclic voltammetry for nickel powders in alkaline solutions [30] as the catalytic activity can also be affected by other factors such as porosity and shape of the particles.

We were not able to obtain the same size particles for all metals. On the basis of the same weight of materials, however, SS 316 (16 μm) and NiO_x 87302 (74 μm) had higher overpotentials than nickel (0.5–7 μm), electrodeposited nickel (0.001 μm), or plain CB (Table 1). On the basis of similar calculated surface areas (0.001–0.002 m^2), NiO_x 87302 had higher overpotentials than any of the stainless steels (150 μm) tested and CB. SS 316–16 um had higher overpotentials than SS 316–150 μm (lower surface area) and Ni 10256 (similar surface area).

Stainless steel 304 (140 μm) had lower overpotentials at −3.2 log A/cm^2 than the other stainless steel materials tested, with overpotentials increasing in the order SS 304, SS 316, SS 410 and SS 303. This finding is consistent with our previous MEC study where sheet metal cathodes made from SS 304 performed better than other stainless steels and nickel alloys [21]. In that study, however, overpotentials of MEC cells with used cathodes made of SS 304 were similar to overpotentials of SS 316 (SS 410 and SS 303 were not tested). The difference in overpotentials observed between these two studies could be due to particle geometry, interactions with the binder, effect of microbes and use.

3.2. *MEC performance*

The two metal powder and binder combinations that produced the lowest overpotentials in LSV scans (Ni 210 with 267 μL Nafion, and Ni 210 + CB with 400 μL Nafion) (Table 1) were used as cathodes in MECs, and their performance was compared to the same reactors with Pt cathodes. Electrodeposited nickel oxide ($eNiO_x$) was also chosen as an MEC cathode due to its good performance in a previous study [21]. The resulting BET total surface areas were 4.31 m^2/g (Ni 210), 11.8 m^2/g (Ni 210 + CB), 17.3 m^2/g ($eNiO_x$), and 11.2 m^2/g (Pt).

3.2.1. *Volumetric gas production and composition*

The MECs with two nickel cathodes (Ni 210 and Ni 210 + CB) produced gas similar in volume and composition to that obtained with Pt cathodes, but the performance was different for the $eNiO_x$ cathode (Table 2, Fig. 2). Although the volume of gas produced was initially similar for all these electrodes, the volume of gas decreased for reactors with the $eNiO_x$ catalyst after 12 cycles compared to the Ni and Pt catalysts (Fig. 2A). Gas composition was always very similar for all cathodes, with 92% H_2 for the Ni and Pt catalysts, and 94% H_2 for $eNiO_x$ (Table 2).

3.2.2. *Current production*

The maximum current produced with Pt cathodes (5.6–6.3 mA) (Fig. 2B) was larger than with the other cathodes, and performance was consistent over 12 MEC cycles. The length of the cycle time increased in the following order: Pt, Ni 210 (with and without CB) and eNiOx. For example, the time to reach the same low voltage of 0.02 V was 5–10 h longer for Ni 210 than Pt depending on the specific cycle. The maximum current increased for the two Ni cathodes over the first 6 cycles by as much as 4.7 mA for Ni 210, and 4.1 mA for Ni 210 + CB. The current decreased by 3.3 mA, however, for $eNiO_x$ over the same 6 cycles (Fig. 2B). The change in these maximum current densities indicated that the systems had not reached stable and steady conditions. There are a number of factors that could affect changes in the current densities over these cycles, including the possibility that the characteristics of the bacterial biofilm or microbial community was changing, or changes in cathode surface area due to metal oxidation or to separation of particles from the carbon cloth support.

Table 2 – Summary of MEC results for Ni 210, Ni 210 + CB, eNiOx and Pt catalyst cathodes at an applied voltage of 0.6 V, eighth cycle of operation.

Metal	H_2 (%)	I_v (A/m^3)	Q (m^3/m^{3}d)	CE (%)	$r_{H_2,cat}$ (%)	$r_{H_2,COD}$ (%)	η_E (%)	η_{E+S} (%)
Ni 210	92 ± 0	160 ± 31	1.3 ± 0.3	92.7 ± 15.8	79 ± 10	73 ± 3	210 ± 40	65 ± 2
Ni 210 + CB	92 ± 1	139 ± 2	1.2 ± 0.1	83.8 ± 1.2	94 ± 5	79 ± 5	252 ± 12	73 ± 4
$eNiO_x$	94 ± 0	103 ± 4	0.9 ± 0.1	87.1 ± 2.3	86 ± 1	75 ± 1	215 ± 8	67 ± 0
Pt	92 ± 2	186 ± 4	1.6 ± 0.0	85.0 ± 6.4	89 ± 7	75 ± 0	239 ± 21	70 ± 2

However, following the sixth cycle all the cathodes showed repeatable maximum current densities.

3.2.3. *Coulombic efficiency, recoveries and hydrogen production rates at 0.6 V*

Coulombic efficiency, cathodic recovery, hydrogen recovery, energy recovery based on electrical input or overall energy recovery were the same (within ±1 S.D.) for all cathodes used in MECs. These parameters are not directly correlated to each other because they are calculated for different parts of the cycle. For example, I_v and Q were based on the initial maximum current (averaged over a period of 2 h), while coulombic efficiency was calculated from the measured current over a complete cycle. As cycle times were longer with Ni 210 cathodes, it was possible to obtain higher values for *CE*s but lower I_vs for MECs with Ni 210 compared to those with Pt cathodes. The only MEC performance parameter that varied among the tested cathodes was the hydrogen production rate. The production rate was slightly lower for Ni 210 (Q = 1.2–1.3 m^3/m^3/d) than for Pt (Q = 1.6 m^3/m^3/d) even though gas production and composition was similar for Pt and Ni 210 cathodes (Fig. 2A). This lower production rate follows the lower maximum current density produced with Ni 210 (139–160 A/m^3) than with Pt (186 A/m^3) (Table 2). Q was lower for $eNiO_x$ than the other cathodes due to both a lower gas production rate and lower maximum current density (103 A/m^3).

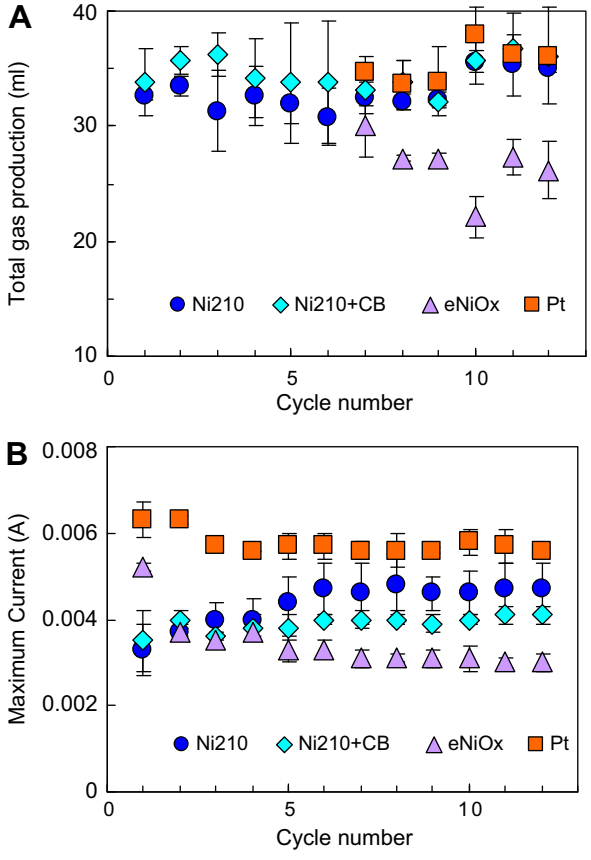

Fig. 2 – (A) Total gas production and (B) maximum current for MECs with Ni 210, Ni 210 + CB, $eNiO_x$ or Pt catalyst cathodes, as a function of cycle number at an applied voltage of 0.6 V. Gas production for cycles 1–6 were not recorded for Pt and $eNiO_x$ due to equipment malfunction.

3.2.4. *MEC performance with Ni 210 cathodes as a function of applied voltage*

Hydrogen production rates with the two Ni cathodes increased with applied voltage and were not significantly different from each other, with the largest rates produced at the highest applied voltage of 0.8 V (Q = 1.85 m^3/m^3/d, Ni 210) (Fig. 3A). There was no hydrogen production with the Ni catalysts at an applied voltage of 0.3 V, compared to 0.2 V previously observed with a Pt catalyst [23]. Coulombic efficiencies (*CE*) decreased slightly with applied voltage (89% at 0.8 V, to 81% at 0.4 V) (Fig. 3B). Cathodic hydrogen recovery reached a maximum at 0.7 V (Ni 210 = 93%, Ni 210 + CB = 91%). Similarly, energy recovery based on electrical input (η_E) and overall energy recovery (η_{E+S}) increased with increasing applied voltage, with the maximum values for η_E at 0.8 V of 240%, and for η_{E+S} at 0.7 V of 74%.

3.3. *Cathode catalytic activity and surface analysis of used cathodes*

The performance of the cathodes decreased after use in an MFC. Following 12 MEC cycles of operation, the "used" cathodes were again analyzed by LSV (Fig. 4) and by SEM (Fig. 5). LSV scans for both Ni 210 and Pt decreased in performance to similar overpotentials. For example, the overpotentials at −3.2 log A/cm^2 increased to −0.733 V for used Ni 210 and −0.713 V for used Pt, compared to −0.500 V for the new cathodes. The largest change in overpotential was observed for the used $eNiO_x$ cathodes, which increased to −1.043 V compared to −0.800 V for new cathodes. The LSV for the used Ni 210 + CB cathodes exhibited the least change following use in an MEC, with final overpotentials between those of Ni 210 and $eNiO_x$.

The surfaces of the Ni 210-based cathodes observed using SEM showed very similar structures before and after 12 MEC cycles, both with (Fig. 5A and B) and without CB (not pictured). $eNiO_x$ had finer structures before use (Fig. 5C) but broader

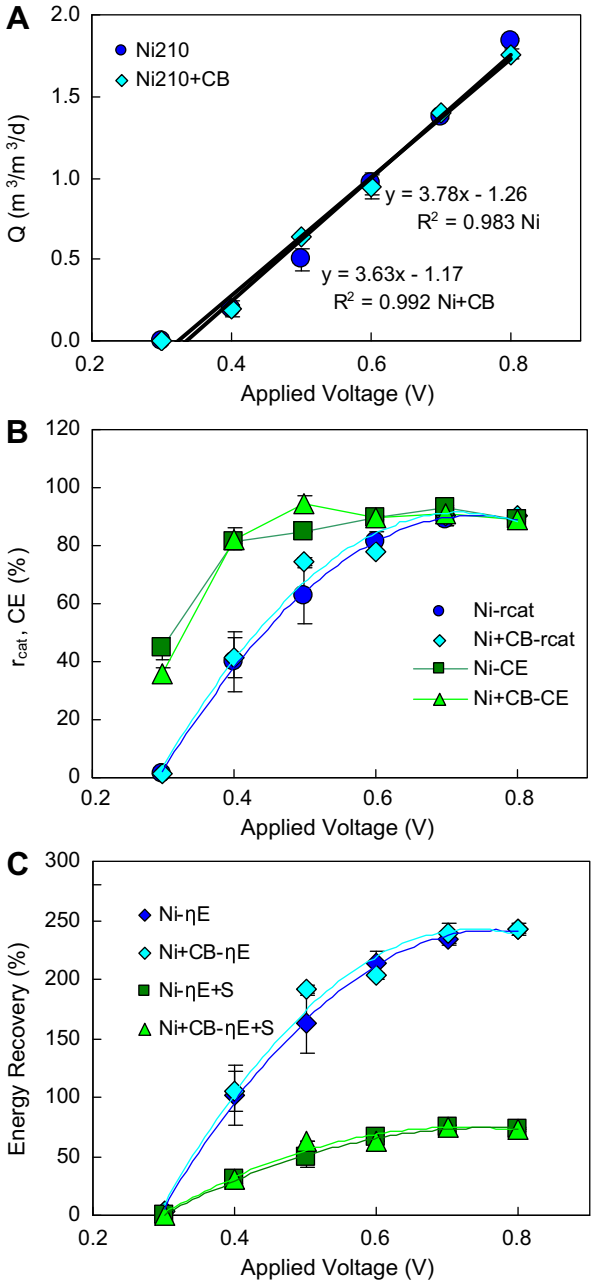

Fig. 3 – MEC performance for Ni 210 catalyst cathodes at different applied voltages. (A) hydrogen production rate (B) cathodic recovery and coulombic efficiency (C) energy recovery based on electrical input and overall energy recovery.

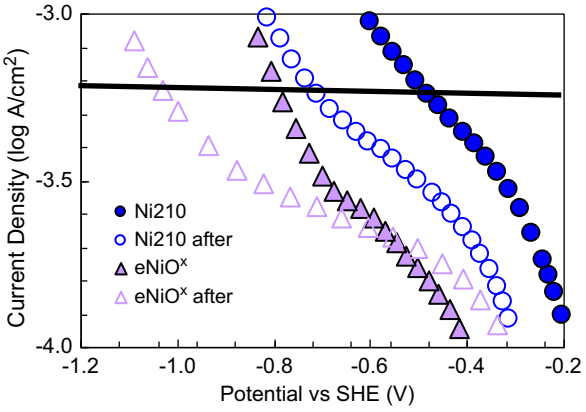

Fig. 4 – Examples of Tafel plots for cathodes before and after use in 12 MEC cycles. Test conditions: 2 mM phosphate buffer, scan rate 2 mV/s, third scan.

geometries and less material after use (Fig. 5D), suggesting a loss of the nickel oxide material.

3.4. *Nickel stability*

It was hypothesized that the decreased performance of the nickel cathodes was due to corrosion and Ni dissolution. Ni concentrations in solution were therefore measured over 12 cycles (Fig. 6A). The Ni concentration with the Ni 210 cathode was 4.9 ± 0.8 ppm, with lower concentrations for the Ni 210 + CB (4.1 ± 1 ppm) and $eNiO_x$ (1.67 ± 0.29 ppm). These values are substantially larger than that expected based on Ni added into the medium (0.01 ppm) or the concentration measured in medium with the Pt cathodes (0.115 ± 0.007 ppm). A loss of Ni due to corrosion was also indicated by changes in BET surface areas, with decreases from 4.31 (new) to 3.84 m^2/g (used) for the Ni 210 cathodes, and 11.83 (new) to 7.81 m^2/g (used) for the Ni 210 + CB cathodes. BET areas are not only affected by the catalyst, however, but also by the presence of CB, binder, or other materials that accumulated on the catalyst surface.

The standard procedure for changing the medium consisted of exposing the electrodes to air for 15 min (to reduce methanogen growth), but we reasoned this procedure led to Ni corrosion. To test whether this process was responsible for the loss of Ni in solution, after each cycle we replaced the MEC medium in an anaerobic glove box, thus avoiding exposure of the cathodes to air. Under these conditions of continuous anaerobic operation, there was a decrease of Ni in solution over successive cycles, from 5.7–6 ppm in the first cycle to 0.2 ppm (±0.4 ppm, Ni 210; ±0.3 Ni 210 + CB) for the last 6 cycles (Fig. 6B). Some of this dissolved nickel does not originate from the Ni 210 cathode, but likely originates from the water as Ni was also present in the used media from the MECs with Pt cathodes (0.115 ppm Ni). Based on the low concentrations of Ni in solution, we concluded that the primary mechanism of Ni corrosion was due to air exposure during replacement of the medium at the beginning of a fed-batch cycle.

3.5. *Microbial community*

The closest matches to sequences obtained from the anode biofilm from the MEC with a Ni cathode (Fig. 7) were *Pelobacter propionicus* (54.3%) and *Geobacter sulfurreducens* (21.7%), both members of the *δ-proteobacteria* (76.0% total). Other bacteria included *Dechloromonas aromatica* (4.35%), *Chromobacterium violaceum* (6.52%), *Thauera sp MZ1T* (8.69%), *Diaphorobacter sp TPSY* (2.17%) and *Polaromonas naphthalenivorans* (2.17%), all *ß-proteobacteria* (23.9%). These communities were similar to

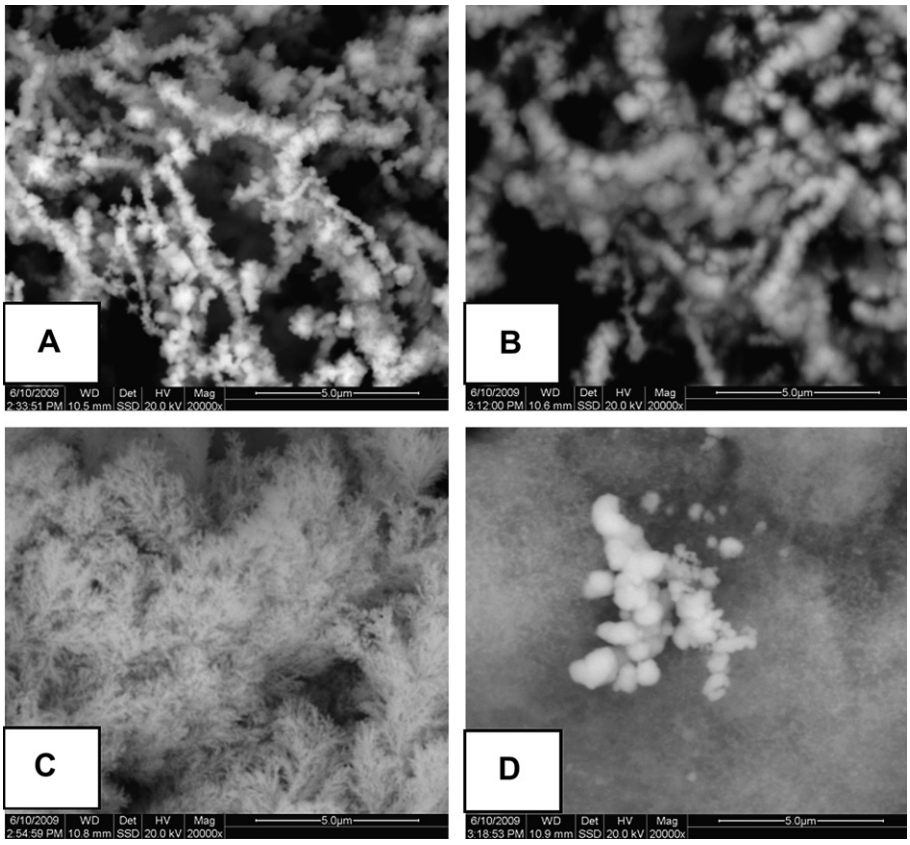

Fig. 5 – SEM images of Ni 210 catalyst cathodes (A and B) and eNiOx catalyst cathodes (C and D), before (A and C) and after (B and D) 12 cycles in MEC. Images are at 20,000 × magnification.

those found in the MEC with a Pt cathode, with *P. propionicus* (56.5%) and *G. sulfurreducens* (39.1%) again dominant in the community (95.6% total) (data not shown). *D. aromatica RCB* (2.2%) was also present, along with *Alkaliphilus oremlandii OhILAs* (2.2%, Firmicutes). These results show that the cathode did not appreciably impact anodic community structure.

4. Discussion

4.1. *Cathode performance*

Ni powder cathodes produced results similar to those obtained with Pt cathodes in MEC tests in terms of coulombic efficiency, cathodic, hydrogen and energy recoveries. The Ni powder cathodes had a smaller calculated surface area (0.60 m^2), measured BET surface area (4.3 m^2/g) and particle sizes of the Ni (0.5–1 μm) than the Pt cathodes (1.45 m^2, 11.2 m^2/g, 0.002 μm). Calculated surface areas, however, do not take into account catalyst interaction with the carbon black (if present) and carbon cloth, coverage by the binder, or particle agglomeration during application which would reduce the electrochemically active surface area. The similar performance of the Ni and Pt cathodes in MEC tests suggests that current densities were limited by factors other than the intrinsic catalytic activity of these metals. LSVs were useful in indicating general trends in MEC performance but cathodes ultimately need to be tested in MECs due to additional effects that are not measured during electrochemical testing, such as microbial interference or catalyst degradation.

There was loss of nickel when the MEC was aerated between cycles, as shown by elevated nickel concentrations in solution compared to the medium, and decreased BET surface areas. When exposed to air, a nickel oxide layer forms that is 3–5 monolayers thick [31]. Outer layers of nickel can become hydroxylated, forming $Ni(OH)_2$ in water, and may dissolve unless the metal is kept under alkaline conditions. If the MEC reactor was operated in batch mode, it would take 444 fed-batch cycles under the conditions examined here to dissolve the Ni on the cathode (60 mg) assuming an average loss of 4.5 ppm Ni per cycle in a 30 ml reactor. Based on fed-batch cycle times, this would mean that the cathode would need to be replaced after about a year. Nickel is naturally present in the environment, it is an essential micronutrient, and it is not listed as a toxic chemical by the EPA as there is no maximum level set for drinking water. Nickel is primarily a respiratory toxic metal [32] and can produce allergic reactions, chronic toxicity and respiratory tract cancer. One study showed no cancer tumors in mammalians which received Ni(II) compounds in drinking water [32], but another study showed gill damage in juvenile trout at waterborne Ni concentrations of 15.3 ± 2.6 ppm [33]. These concentrations are 3.4 times higher than the average Ni value measured in this study (4.5 ppm).

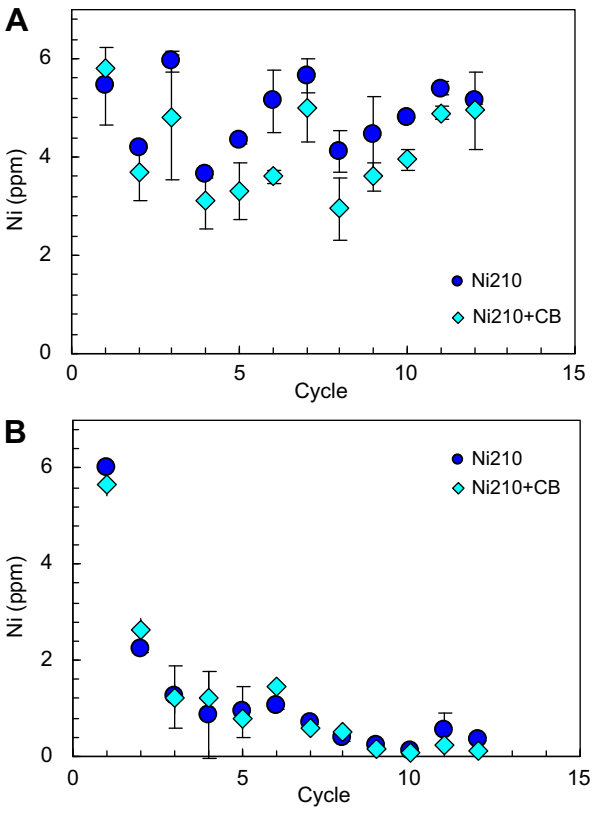

Fig. 6 – Nickel content via ICP-AES analysis in MEC solution after (A) aerobic feeding and (B) anaerobic feeding.

Nickel powder was relatively stable with respect to corrosion when MECs were continuously maintained under anaerobic conditions. Constant gas and current production over 12 cycles of MEC operation, a similarity of overpotentials between Ni 210 and Pt cathodes both before and after use, and a similarity of SEM images before and after use also support the stability of the metal in the Ni 210 cathode. Ni dissolution would not be an issue during large scale applications if the MEC was operated continuously, especially as the localized pH of the cathode could be alkaline [23,34,35]. However, a lack of aeration could increase methane production. During this study, the methane in the gas increased from 0% to 15.2 ± 3.9% for Ni 210, and to 4.4 ± 3.9% for Ni 210 + CB by the eighth cycle when the MECs were not exposed to air between feedings. Techniques to decrease methane production, other than aeration, need to be explored to minimize corrosion of cathodes made with nickel powders (and potentially other metals).

There was a linear increase in hydrogen production rate with applied voltage, consistent with previous MEC studies using Pt catalysts [4,23,26]. There was no measured hydrogen production, and only a very small current, with the Ni 210 catalysts at an applied voltage of 0.3 V, compared to the lower value of 0.2 V previously observed with a Pt catalyst in a similar setup [23]. Hydrogen evolution may not be occurring at this low potential with Ni. Ni has a lower exchange current density and binds hydrogen atoms less strongly than Pt [36]. This suggests that lower current densities (and therefore lower hydrogen production) would occur with Ni than Pt at the same applied potential, based on predictions using the Tafel expression

$$\log J = \log J_0 + \frac{\alpha_c n_e F}{2.303RT}(E - E_0) \quad (2)$$

where J (A/cm^2) is the current density, J_0 (A/cm^2) the exchange current density, α_c the cathodic transfer coefficient, n_e the number of electrons per reaction (2 for hydrogen), $(E-E_0)$ (V) the overpotential, F Faraday's constant (96,485 C/mol electrons), and R the gas law constant (8.3145 J/mol/K) (assuming that α_c is independent of the metal). As the applied potential increases, the reaction rate at the surface increases and the transport of the species to or from the surface can become the rate limiting step. The type of metal used as the catalyst will not affect the rate of hydrogen evolution once it becomes mass transfer limited. Mass transfer limitated hydrogen evolution likely occurred at an applied voltage of 0.6 V, as the performance of the MECs was the same with either Pt or Ni cathodes at this voltage. Mass transfer limited transport could also be the reason that the amount of Ni 210 metal loading (between 60

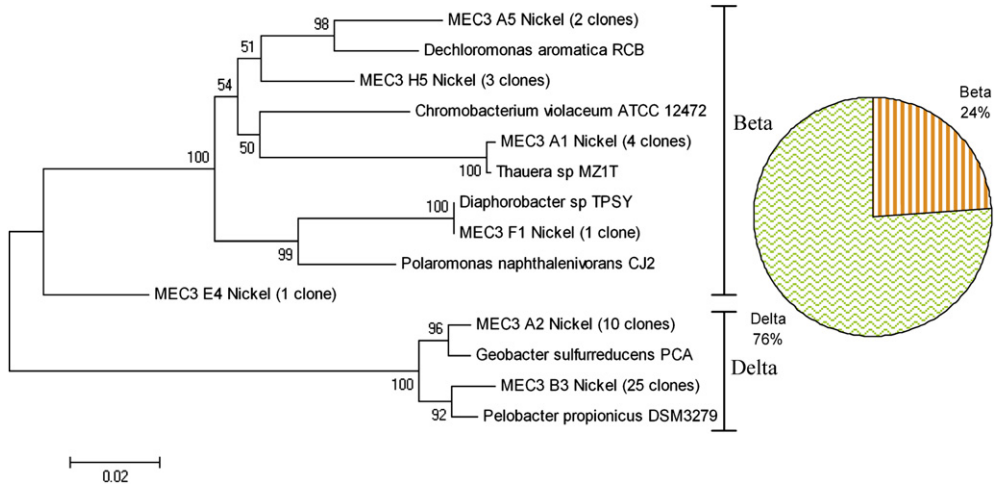

Fig. 7 – Microbial community and phylogenic distances to closest match based on 16S rRNA sequences recovered from the MEC anode with Ni 210 catalyst cathode.

and 90 mg) did not affect overpotentials in LSV tests. It has previously been observed that potentials produced with cathodes prepared similarly to the ones used here (carbon cloth, Nafion, catalyst) did not vary significantly with Pt loading (0.1–2 mg/cm^2) in chronopotentiometry tests (measure cathode potential by applying a constant current) [37]. This is a different effect than in hydrogen fuel cells where the performance is greatly affected by Pt loading [38]. The overpotentials needed to transition from kinetic limiting conditions to mass transport limiting conditions are system dependent.

4.2. *Microbial community*

The anodic microbial community was very similar for MECs with Ni 210 and Pt cathodes, indicating the cathodes did not affect development of the community on the anode. The communities of the MECs were mostly comprised of *Geobacteraceae* (21.7–39.1% *G. sulfurreducens* and 54.3–56.5% *P. propionicus*) and other anaerobes, except for *Polaromonas naphthalenivorans* which is an aerobe heterotroph. Other acetate-fed Pt-cathode MEC reactors with phosphate buffer were similarly found to be dominated by *Geobacteraceace* (16% *Geobacter* sp., 56% *P. propionicus*) [39], while 2-chamber MECs with carbonate buffer were dominated by *Shewanella* and *Pseudomonas* [40].

G. sulfurreducens was the only known exoelectrogen [41] present from the bacteria identified in these MECs, and therefore the role of the other microbes in the biofilm is unclear. The most abundant bacterium identified in the MECs was *P. propionicus* which is not known to oxidize acetate and has been shown to be incapable in electron transfer to metals or electrodes [42]. *Pelobacter* sp. may have a fermentative or syntrophic role with *Geobacter* sp. that has to be further studied, similar to syntrophic interactions in microbial fuel cells between exoelectrogens and non-exoelectrogens [43,44].

4.3. *Cathode costs*

The cost of the nickel used in the cathode is orders of magnitude less than the cost of the platinum, resulting in a total cost for catalyst that would be small compared to the costs of other cathode materials. Ni 210 at a loading of 60 mg per 7 cm^2 would cost \$2.82/m^2 compared to \$700/m^2 for the platinum loading used here (calculations based on our purchase prices). At this low cost for the Ni catalyst, the cost of the Nafion binder becomes the main economic consideration as a loading of 267 μL per 7 cm^2 of Nafion costs \$500/m^2. Carbon cloth was also very expensive (\$850/m^2), but this cost could probably be reduced. For example, carbon mesh in bulk costs only \$25/m^2. While carbon mesh has been successfully used as an anode [45], it was indicated that it was too porous to be used for the cathode with current preparation techniques. Additional research is therefore needed to find alternatives for the other cathode components as the cost of the Ni catalyst would be a small percentage of the total cathode cost.

5. Conclusions

Ni powders showed similar performance to Pt powders when used as catalysts in MEC cathodes made with carbon cloth and a Nafion binder. The stability of Ni powders was demonstrated by consistent current densities in LSV scans before and after use of cathodes in MECs over 12 cycles (12 days), as well as by visual analysis of particles in SEM scans and measurements of nickel concentrations in MECs kept under fully anoxic conditions. Avoiding exposure of the Ni catalyst to air was essential for avoiding nickel corrosion and dissolution but increased methane production. Analysis of the anodic biofilms in the MECs showed that *Geobacter sulfurreducens* and *Pelobacter propionicus* were the most abundant bacteria on the anode surface in MECs and that this community was not affected by the use of either Pt or Ni cathode catalysts.

Acknowledgements

The authors thank R. Wagner, P. Kiely, T. Saito, M. Mehanna, S. Cheng and D. Jones for assistance with microbiology, electrochemistry and MEC experiments, and M.J. Janik, J.M. Perez and W.A. Lloyd for their advice and insight. This research was supported by Award KUS-I1-003-13 by King Abdullah University of Science and Technology (KAUST).

REFERENCES

[1] Manish S, Banerjee R. Comparison of biohydrogen production processes. Int J Hydrogen Energy 2008;33:279–86.
[2] Logan BE, Call D, Cheng S, Hamelers HVM, Sleutels THJA, Jeremiasse AW, et al. Microbial electrolysis cells for high yield hydrogen gas production from organic matter. Environ Sci Technol 2008;42:8630–40.
[3] Rozendal RA, Hamelers HVM, Euverink GJW, Metz SJ, Buisman CJN. Principle and perspectives of hydrogen production through biocatalyzed electrolysis. Int J Hydrogen Energy 2006;31:1632–40.
[4] Tartakovski B, Manuel MF, Wang H, Guiot SR. High rate membrane-less microbial electrolysis cell for continuous hydrogen production. Int J Hydrogen Energy 2009;34:672–7.
[5] Rozendal RA, Hamelers HVM, Rabaey K, Keller J, Buisman CJN. Towards practical implementation of bioelectrochemical wastewater treatment. Trends Biotechnol 2008;26:450–9.
[6] Call DF, Merrill MD, Logan BE. High surface area stainless steel brushes as cathodes in microbial electrolysis cells. Environ Sci Technol 2009;43:2179–83.
[7] Hu H, Fan Y, Liu H. Hydrogen production in single-chamber tubular microbial electrolysis cells using non-precious-metal catalysts. Int J Hydrogen Energy 2009; Available online:doi:10.1016/j.ijhydene.2009.08.011.
[8] Lee HS, Torres CI, Parameswaran P, Rittman BE. Fate of H_2 in an upflow single-chamber microbial electrolysis cell using a metal-catalyst-free cathode. Environ Sci Technol 2009;43:7971–6.
[9] Rozendal RA, Jeremiasse AW, Hamelers HVM, Buisman CJN. Hydrogen production with a microbial biocathode. Environ Sci Technol 2008;42:629–34.
[10] Harnish F, Sievers G, Schröder U. Tungsten carbide as electrocatalyst for the hydrogen evolution reaction in pH neutral electrolyte solutions. Appl Catalysis B: Env 2009;89:455–8.
[11] Couper AM, Pletcher D, Walsh FC. Electrode materials for electrosynthesis. Chem Rev 1990;90:837–65.
[12] Salgado JRC, Andrade MHS, Silva JCP, Tonholo J. A voltammetric study of α- and β-hydroxides over nickel alloys. Electrochim Acta 2002;47:1997–2004.

[13] Jakšić JM, Vojnović MV, Krstajić NV. Kinetic analysis of hydrogen evolution at Ni–Mo alloy electrodes. Electrochim Acta 2000;45:4151–8.
[14] Highfield JG, Claude E, Oguro K. Electrocatalytic synergism in Ni/Mo cathodes for hydrogen evolution in acid medium: a new model. Electrochim Acta 1999;44:2805–14.
[15] Kedzierzawski P, Oleszak D, Janik-Czachor M. Hydrogen evolution on hot and cold consolidated Ni–Mo alloys produced by mechanical alloying. Mat Sci Eng 2001;A300: 105–12.
[16] Daftsis E, Pagalos N, Jannakoudakis A, Jannakoudakis P, Theodoridou E, Rashkov R, et al. Preparation of a carbon fiber-nickel-type material and investigation of the electrocatalytic activity for the hydrogen evolution reaction. J Electrochem Soc 2003;150:C787–93.
[17] Olivares-Ramírez JM, Campos-Cornelio ML, Uribe Godínez J, Borja-Arco E, Castellanos RH. Studies on the hydrogen evolution reaction on different stainless steels. Int J Hydrogen Energy 2007;32:3170–3.
[18] Marcelo D, Dell'Era A. Economical electrolyser solution. Int J Hydrogen Energy 2008;33:3041–4.
[19] Haryanto A, Fernando SD, Filip To SD, Steele PH, Pordesimo L, Adhikari S. Hydrogen production through the water-gas shift reaction: thermodynamic equilibrium versus experimental results over supported Ni catalysts. Energy Fuels 2009;23:3097–102.
[20] Adhikari S, Fernando SD, Haryanto A. Hydrogen production from glycerin by steam reforming over nickel catalysts. Renewable Energy 2008;33:1097–100.
[21] Selembo PA, Merrill MD, Logan BE. The use of stainless steel and nickel alloys as low-cost cathodes in microbial electrolysis cells. J Power Sources 2009;190:271–8.
[22] Merrill MD, Dougherty RC. Metal oxide catalysts for the evolution of O_2 from H_2O. J Phys Chem C 2008;112: 3655–66.
[23] Call D, Logan BE. Hydrogen production in a single chamber microbial electrolysis cell lacking a membrane. Environ Sci Technol 2008;42:3401–6.
[24] Logan BE, Cheng S, Watson V, Estadt G. Graphite fiber brush anodes for increased power production in air-cathode microbial fuel cells. Environ Sci Technol 2007;41:3341–6.
[25] Cheng S, Logan BE. Ammonia treatment of carbon cloth anodes to enhance power generation of microbial fuel cells. Electrochem Comm 2007;9:492–6.
[26] Cheng S, Logan BE. Sustainable and efficient biohydrogen production via electrohydrogenesis. Proc Natl Acad Sci 2007; 104:18871–3.
[27] Lalaurette E, Thammannagowda S, Mohagheghi A, Maness PC, Logan BE. Hydrogen production from cellulose in a two-stage process combining fermentation and electrohydrogenesis. Int J Hydrogen Energy 2009;34: 6201–10.
[28] Liu H, Logan BE. Electricity generation using an air-cathode single chamber microbial fuel cell in the presence and absence of a proton exchange membrane. Environ Sci Technol 2004;38:2281–5.
[29] Hitz C, Lasia A. Experimental study and modeling of impedance of the her on porous Ni electrodes. J Electroanalytical Chem 2001;500:213–22.
[30] Zhao X, Ding Y, Ma L, Shen X, Xu S. Structure, morphology and electrocatalytic characteristics of nickel powders treated by mechanical milling. Int J Hydrogen Energy 2008;33:6351–6.
[31] Hernández N, Moreno R, Sánchez-Herencia AJ, Fierro JLG. Surface behavior of nickel powders in aqueous suspensions. J Phys Chem B 2005;109:4470–4.
[32] Kasprzak KS, Sunderman FW, Salnikow K. Nickel carcinogenesis. Mutat Res 2003;533:67–97.
[33] Pane EF, Richards JG, Wood CM. Acute waterborne nickel toxicity in the rainbow trout (Oncorhynchus mykiss) occurs by a respiratory rather than ionoregulatory mechanism. Aquat Toxicol 2003;63:65–82.
[34] Rozendal RA, Hamelers HVM, Molenkamp RJ, Buisman CJN. Performance of single chamber biocatalyzed electrolysis with different types of ion exchange membranes. Water Res 2007;41:1984–94.
[35] Sleutels THJA, Hamelers HVM, Rozendal RA, Buisman CJN. Ion transport resistance in microbial electrolysis cells with anion and cation exchange membranes. Int J Hydrogen Energy 2009; doi:10/1016/j.ijhydene.2009.03.004.
[36] Conway BE, Jerkiewicz G. Nature of electrosorbed H and its relation to metal dependence of catalysis in cathodic H_2 evolution. Solid State Ionics 2002;150:93–103.
[37] Cheng S, Liu H, Logan BE. Power densities using different cathode catalysts (Pt and CoTMPP) and polymer binders (Nafion and PTFE) in single chamber microbial fuel cells. Environ Sci Technol 2006;40:364–9.
[38] Qi Z, Kaufman A. Low Pt loading high performance cathodes for PEM fuel cells. J Power Sources 2003;113:37–43.
[39] Chae KJ, Choi MJ, Lee J, Ajayi FF, Kim IS. Biohydrogen production via biocatalyzed electrolysis in acetate-fed bioelectrochemical cells and microbial community analysis. Int J Hydrogen Energy 2008;33:5184–92.
[40] Liu W, Wang A, Ren N, Zhao X, Liu L, Yu Z, et al. Electrochemically assisted biohydrogen production from acetate. Energy Fuels 2008;22:159–63.
[41] Logan BE. Exoelectrogenic bacteria that power microbial fuel cells. Nat Rev Microbiol 2009;7:375–81.
[42] Butler JE, Young ND, Lovley DR. Evolution from a respiratory ancestor to fill syntrophic and fermentative niches: comparative fenomics of six Geobacteraceae species. BMC Genomics 2009;10:103.
[43] Freguia S, Rabaey K, Yuan Z, Keller J. Syntrophic processes drive the conversion of glucose in microbial fuel cell anodes. Environ Sci Technol 2008;42:793–7943.
[44] Parameswaran P, Torres CI, Lee HS, Krajmalnik-Brown R, Rittman BE. Syntrophic interactions among anode respiring bacteria (ARB) and non-ARB in a biofilm anode: electron balances. Biotechnol Bioeng 2009;103:513–23.
[45] Wang X, Cheng S, Feng Y, Merrill MD, Saito T, Logan BE. Use of carbon mesh anodes and the effect of different pretreatment methods on power production in microbial fuel cells. Environ Sci Technol 2009;43:6870–4.